ECOGRAPHY

Research

Quantifying the climatic niche of symbiont partners in a lichen symbiosis indicates mutualist-mediated niche expansions

Gregor Rolshausen, Francesco Dal Grande, Anna D. Sadowska-Deś, Jürgen Otte and Imke Schmitt

G. Rolshausen (http://orcid.org/0000-0003-1398-7396) (grolshausen@senckenberg.de), F. Dal Grande, A. D. Sadowska-Deś, J. Otte and I. Schmitt, Senckenberg Biodiversity and Climate Research Centre (SBiK-F), Frankfurt am Main, Germany. ADS-D and IS also at: Dept of Biological Sciences, Inst. of Ecology, Evolution and Diversity, Goethe Univ., Frankfurt, Germany.

The large distributional areas and ecological niches of many lichenized fungi may in part be due to the plasticity in interactions between the fungus (mycobiont) and its algal or cyanobacterial partners (photobionts). On the one hand, broad-scale phylogenetic analyses show that partner compatibility in lichens is rather constrained and shaped by reciprocal selection pressures and codiversification independent of ecological drivers. On the other hand, sub-species-level associations among lichen symbionts appear to be environmentally structured rather than phylogenetically constrained. In particular, switching between photobiont ecotypes with distinct environmental preferences has been hypothesized as an adaptive strategy for lichen-forming fungi to broaden their ecological niche. The extent and direction of photobiont-mediated range expansions in lichens, however, have not been examined comprehensively at a broad geographic scale. Here we investigate the population genetic structure of *Lasallia pustulata* symbionts at sub-species-level resolution across the mycobiont's Europe-wide range, using fungal *MCM7* and algal ITS rDNA sequence markers. We show that variance in occurrence probabilities in the geographic distribution of genetic diversity in mycobiont-photobiont interactions is closely related to changes in climatic niches. Quantification of niche extent and overlap based on species distribution modeling and construction of Hutchinsonian climatic hypervolumes revealed that combinations of fungal–algal interactions change at the sub-species level along latitudinal temperature gradients and in Mediterranean climate zones. Our study provides evidence for symbiont-mediated niche expansion in lichens. We discuss our results in the light of symbiont polymorphism and partner switching as potential mechanisms of environmental adaptation and niche evolution in mutualisms.

Introduction

Associations between species in obligate mutualisms, such as lichens or corals, evolve under two main sets of constraints: a broad-scale phylogenetic component, determined by the general compatibility of host genera with their symbiotic partners; and a local-scale ecological component determined by adaptive dynamics, environmental

tolerances, and dispersal abilities of partners in the symbiosis. For instance, the majority of lichen-forming fungi (mycobionts) in nature are known to be exclusively associated with particular genera of autotrophic photobionts (i.e. *Trebouxia* algae or *Nostoc* cyanobacteria), suggesting an inherent deep phylogenetic constraint in partner compatibility (Beck et al. 1998, Rambold et al. 1998, Piercey-Normore and DePriest 2001, DePriest 2004). Likewise, comprehensive analyses of symbiont associations in the species-rich lichen family Parmeliaceae revealed that, at the scale of ecoregions, the fungal host genus determines the composition of photobionts more than ecological predictors (Leavitt et al. 2015).

At the level of species, however, and especially at the level of populations, the phylogenetic specificity of associating lichen partners appears to be less stringent. On the one hand, several mycobiont species may associate with the same photobiont species, often forming so called lichen guilds (e.g. cyanobacteria: Rikkinen et al. 2002, Wirtz et al. 2003, green algae: Doering and Piercey-Normore 2009, Dal Grande et al. 2014, Singh et al. 2017). On the other hand, a particular mycobiont can associate with multiple strains of photobionts, as well as switch between those strains within its distributional range (Piercey-Normore and DePriest 2001, Blaha et al. 2006, Piercey-Normore 2006, Yahr et al. 2006, Muggia et al. 2010). Moreover, photobionts are not exclusively transmitted vertically during propagation and reproduction of their mycobiont partners, but can also be transmitted horizontally between mycobionts (Friedl 1987, Piercey-Normore and DePriest 2001, Werth and Sork 2008, 2010) and potentially even occur free-living (Mukhtar et al. 1994, Beck et al. 1998). Thus, while environmental preferences in lichen photobionts can evolve independently of a particular mycobiont, the spatial distribution and (realized) niche breadth of lichen-forming fungi will inherently depend on the adaptation of their photobionts to local environmental conditions (Piercey-Normore and DePriest 2001, Yahr et al. 2006, Fernández-Mendoza et al. 2011).

Evidence that association with differentially adapted photobionts alters the niche breadth of lichen-forming fungi comes from explicit phylogeographic approaches that relate the congruency in genetic structures of symbiotic partners to their geographic distributions. A common pattern found in studies addressing this question is that the fungal partner often exhibits substantially less genetic structure at the subspecies level across habitats compared to its photobiont partners; thereby suggesting a generalist strategy in the former, and a central role for local adaptation in the latter (Piercey-Normore 2006, Yahr et al. 2006, Werth and Sork 2008, 2010, Widmer et al. 2012, Muggia et al. 2014). Moreover, horizontal transfer of photobionts of the genus *Trebouxia* or the genus *Asterochloris* between different populations of mycobionts seems to have occurred with high ecological specificity both at a local-scale (Piercey-Normore 2006, Werth and Sork 2010, Peksa and Ŝkaloud 2011) and at larger scales of ecogeographic regions (Yahr et al. 2006, Fernández-Mendoza et al. 2011, Werth and Sork 2014). By and large,

inferences in these studies are drawn from methods that aim at 1) explaining the molecular variance observed for a particular taxonomic group (i.e. photobionts or mycobionts) via categorical predictors for habitat and/or symbiotic partners (e.g. F_{ST} and AMOVA methods, Werth and Sork 2008, 2010); 2) evaluating phylogenetic correspondence between associated symbiotic partners and habitat (e.g. Mantel tests and phylogenetic signal; Yahr et al. 2006, Peksa and Ŝkaloud 2011, Singh et al. 2017); or 3) partitioning presence/absence variation for particular symbiont haplotypes onto environmental variables (e.g. redundancy analysis; Fernández-Mendoza et al. 2011, Werth and Sork 2014). Yet, while these approaches do consider environmental variables as predictors for the distribution of molecular variance, none of them places special emphasis on explicitly quantifying the niche breadth of, or the niche overlap between, symbiotic partners.

If mycobionts broaden their distributional range by associating with differently adapted photobionts, we would expect to find a patchwork of genetically differentiated populations of interacting partners throughout that range. Moreover, we expect such a geographic mosaic of interactions to be structured by the mode of dispersal (and reproduction) of partners, as well as by their capabilities to adapt to spatially varying selection regimes (Thompson 1999, 2005). More specifically, in the case of predominantly vertical transmission of photobionts (i.e. no algal switches) during mycobiont reproduction and dispersal, the spatial genetic structure of partners should be congruent throughout the geographic mosaic. In contrast, if algal switches are frequent, the spatial genetic structure of partners should be incongruent, resembling a broad generalistic distribution for mycobionts associating with distinct, locally restricted, photobionts (Werth and Sork 2010, Fernández-Mendoza et al. 2011, Dal Grande et al. 2012, O'Brien et al. 2013). Notably, these scenarios should also translate into distinct patterns of overlap in (climatic) niche space among genetically differentiated symbiont partners, given that their observed ecological preferences are the result of adaptation. Thus, modeling niche dimensions (and spatial distributions) for photobionts and mycobionts respectively will provide a more detailed picture of potential coevolutionary 'hotspots', where reciprocal selection between partners is strong, and 'coldspots', where reciprocal selection is weak or absent throughout the lichen's range (Thompson 1999, 2005, Brodie et al. 2002). Furthermore, while there are studies addressing climate change impacts on lichens (Klanderud and Totland 2005, Crabtree and Ellis 2010, Bjerke 2011, Ellis et al. 2014, Lendemer and Allen 2014, Allen and Lendemer 2016), none of them considers environmental preferences of symbiont partners separately. However, assuming that photobiont switches are an adaptive strategy, at least in some lichens (Piercey-Normore and DePriest 2001, Werth and Sork 2008, 2010), and that some photobionts may even occur free-living (Mukhtar et al. 1994, Beck et al. 1998), an important question then arises as to what extent particular photobionts are climatically

suitable in order to facilitate future range shifts in lichens (Ellis 2012).

In the present study, we address the above questions with a model-based framework in the widespread macro-lichen *Lasallia pustulata*, using a comprehensive dataset of presence/absence occurrences throughout the species distributional range, together with a marker-based delineation of sub-species level molecular variance in photobionts and mycobionts (for similar approaches see Gotelli and Stanton-Geddes 2015, Marcer et al. 2016). Despite its predominantly clonal dispersal, *L. pustulata* exhibits a high variability of *Trebouxia* sp. photobionts throughout its range; and most of the *Trebouxia* lineages are shared with other lichen-forming fungi (Sadowska-Deś et al. 2013, 2014), a pattern that suggests frequent switches of photobionts across the species' range. We explore species distribution models (SDMs; Guisan and Zimmermann 2000) together with Hutchinsonian niche hypervolumes (Hutchinson 1957) to ask 1) which climatic factors govern the distribution of photobionts and mycobionts in *L. pustulata* and 2) whether associating with different photobionts influences range expansion of this lichen. Notably, niche quantifications and SDMs calculated from large-scale occurrence data can only give an incomplete description of a species' ecological requirements (or its predicted geographic distribution), because they ignore biotic factors, such as dispersal, competition, and the physiological properties of the organism (Chase and Leibold 2003, Keaney 2006). Our models therefore aim at a dimensional comparison (e.g., uniqueness, extent, overlap) of potential habitat space within a given climatic envelope, rather than at predicting the realized niches of species (Guisan and Zimmermann

2000). Interestingly, however, the quantification of one species' extent in abiotic space (in our study the *Trebouxia* photobionts) can directly correspond to a major biotic niche dimension of another species (in our study the *L. pustulata* mycobionts). Thus, in order to understand potential partner switching strategies, particularly in obligate mutualisms, it is important to quantify the (potential) outcomes of partner switches based on each partner's potential habitat space. To our knowledge, this is the first study approaching the question of preferential photobiont association in lichens from a niche modeling perspective.

Material and methods

Field sampling and molecular methods

We sampled specimens of *L. pustulata* across the species' entire core range, i.e. central Scandinavia to the Canary Islands, and the British Isles to Ukraine and Turkey. In total, we obtained molecular data for 1940 samples (individual thalli) from 119 unique sampling locations (Fig. 1A). Fresh samples were dried and stored at –20°C until DNA extraction. Detailed information about sampling locations and haplotypes are given in Supplementary material Table S1, together with GenBank accession numbers.

From all samples, total genomic DNA was extracted using a small part of the thallus following the CTAB protocol (Cubero and Crespo 2002). Algal symbionts were sequenced at the internal transcribed spacer region nrITS rDNA (primers nrITS1T (f) and nrITS4T (r) based on Kroken and Taylor 2000), and mycobionts were sequenced at the *MCM7*
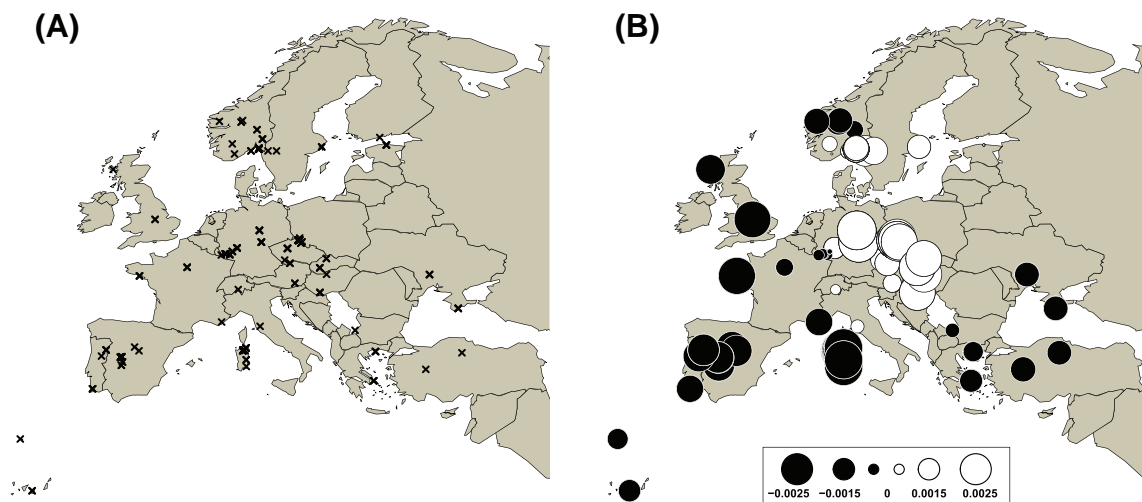

Figure 1. (A) Map depicting 119 unique sampling locations across the core distributional range of *L. pustulata.* (B) Visualization of spatial genetic patterns of *Trebouxia* photobionts using MEMGENE projection (Galpern et al. 2014). Circles represent individual haplotypes. Size and color of the circles depict genetic similarity, with large black and large white circles at opposite extremes of the MEMGENE axis. The legend indicates MEMGENE score values. Visualization of scores for the first MEMGENE axis (explaining 72% of genetic variation among 42 algal haplotypes) suggests the presence of a central genetic cluster (in central Europe) and a peripheral cluster (see Supplementary material Appendix 1 Fig. S1, for the MEMGENE projection of fungal haplotypes).

locus (primers MCM7-709 (f) and MCM7-1348 (r) based on Schmitt et al. 2009). We chose these markers because we have previously shown that they provide the highest intra-population resolution among commonly used sequence-based molecular markers in *L. pustulata* and its associated photobionts (Sadowska-Deś et al. 2013). PCR amplification, amplicon sequencing, and sequence alignment followed established protocols for *L. pustulata* described in Sadowska-Deś et al. (2013, 2014). *Trebouxia* and *Lasallia* sequence identities were confirmed using BLAST searches in GenBank.

Genetic variance and spatial genetic structure

From the aligned sequences, we extracted a total of 42 nrITS rDNA haplotypes for the *Trebouxia* photobionts, and 11 *MCM7* haplotypes for the mycobiont. To characterize the geographic distribution of molecular variance among these haplotypes, we used a regression-based framework to describe the genetic distances – using Kimura's 2-parameter distance – with spatial predictor variables that were generated using Moran's eigenvector maps (MEM; Borcard and Legendre 2002, Griffith and Peres-Neto 2006), as implemented in the 'MEMGENE' R package (Galpern et al. 2014). This approach detects spatial neighborhoods in distance-based data and has been widely used in spatial ecological and genetic contexts (Dray et al. 2012, Manel et al. 2012, Wagner and Fortin 2013, Roffler et al. 2016). The resulting scores for each individual haplotype on the MEM-variables were then used to visualize the spatial genetic structure in our data. Moreover, to examine the genetic variance structure of *Trebouxia* photobionts within and among their fungal partners, we calculated a hierarchical analysis of molecular variance (AMOVA, Excoffier et al. 1992) that considered all algal haplotypes that were associated with one or more of the 11 fungal haplotypes.

Haplotype clustering and OTU delimitation

To circumscribe the molecular variance in our samples for downstream ecological analyses, we used two different approaches to delineate algal and fungal genetic clusters, or operational taxonomic units (hereafter OTUs). Starting from the 42 nrITS rDNA algal haplotypes and the 11 *MCM7* fungal haplotypes respectively, we used the Automatic Barcode Gap Discovery method (ABGD; Puillandre et al. 2012) to delineate photobiont and mycobiont OTUs. Barcode gap discovery infers a model-based confidence limit for intra- and inter-specific genetic distances based on the distribution of all pairwise distances. Depending on this threshold, the method then detects 'barcode gaps' that separate candidate OTUs (Hebert et al. 2003, Puillandre et al. 2012). Notably, the ABGD method has previously been applied to a comprehensive ITS database of *Trebouxia* photobionts from the lichen family Parmeliaceae across a worldwide distribution (Leavitt et al. 2015). In their study, Leavitt et al. (2015) propose a practical ABGD-based classification system for *Trebouxia* photobionts in order to facilitate communication

and consistency across future studies. Thus, we carried out the classification of *Trebouxia* OTUs in our study in accordance with the methods used in Leavitt et al. (2015). For this, genetic distances for the ABGD approach were calculated using the JC69 model, and other parameters were set as follows: Pmin = 0.001, Pmax = 0.01, steps = 10, bins = 20, gap width ranging from 0.1 to 1.5 for consistency assessment of inferred groups. The same settings were used for the *MCM7* data obtained from the mycobionts – although here, no general classification reference for the mycobiont exists. Moreover, in order to investigate the robustness of our algal OTUs, we compared the result of the ABGD delimitation against results from a comprehensive set of alternative delimitation and clustering methods (see Supplementary material Appendix 2, for a detailed description of methods and results of all algal OTU robustness analyses). For downstream analyses, algal and fungal OTUs with too few sampling locations (n < 5) were omitted (see Results).

Niche hypervolumes and species distribution modeling

Delineated clusters/OTUs of photobionts and mycobionts were subjected to two distinct approaches to characterize their respective ecological niches: 1) direct estimation of n-dimensional hypervolumes from observation points (Blonder et al. 2014), and 2) species distribution modeling (SDM) using maximum entropy (MaxEnt, Phillips et al. 2006). We focus on the Hutchinsonian niche concept that describes a species' niche as an n-dimensional hypervolume, where the dimensions are environmental variables, such as climatic variables or resource distributions (Hutchinson 1957). In our study, we describe these environmental dimensions based on a comprehensive set of 12 bioclim variables from the WorldClim dataset (Supplementary material Table S2), drawn at the highest spatial resolution (~1 km) for our sampling area (WorldClim; Hijmans et al. 2005). We chose this restricted but straightforward set of environmental predictor variables to facilitate the interpretation of our models along the main climatic dimensions of temperature and precipitation in wet and dry periods. In addition to the bioclim variable set reported in the main text, we ran all analyses 1) based on the full set of 19 bioclim variables, and 2) based on a reduced set of seven bioclim variables that showed the weakest correlation structure in our dataset. The former set of analyses addresses the issue of variable set completeness, whereas the latter set of analyses addresses issues of collinearity and non-independence among variables (Dormann et al. 2013). We report all results based on the additional variable sets in the supplementary material (i.e. robustness analyses, Supplementary material Appendix 3). Because all results from these robustness analyses of variable sets were highly congruent with the results based on our original variable choice (Supplementary material), we here present results based on the above mentioned set of 12 bioclim variables that facilitate the interpretation of climatic dimensions in our study area.

Based on the aforesaid environmental predictors, we constructed climatic hypervolumes using multivariate kernel

density estimation, described in Blonder et al. (2014). We first condensed the 12 environmental variables into principal component variables (PCs), where PC1–PC2 already described 90% of the total variance. Hypervolumes for each of the photobiont and mycobiont OTUs were then calculated based on n = 5000 random background points across PC1–PC2, applying a range of bandwidth values (0.2–0.8) to test for stability of results. Varying bandwidths did not change the interpretation of our data and we here show results based on a bandwidth of 0.3. To characterize individual differences in climatic preferences among OTUs, reflected by different niche dimensions, we visually examined hypervolume overlaps in niche space. For this, the individual hypervolume of a particular target OTU (fungal or algal) was projected onto the merged hypervolume of the remaining set of OTUs (fungal or algal). The resulting projection in niche space then allows the identification of particular niche dimensions that are uniquely covered by the respective target OTU. Analyses were carried out using the 'hypervolume' R package (Blonder et al. 2014). Notably, the described hypervolume kernel density estimation has been shown to be sensitive to sample sizes and/or environmental dimensionality (Qaio et al. 2016). Thus, in order to test for robustness of our hypervolume analyses, we additionally calculated all niche quantifications based on the approach developed by Broennimann et al. (2012), implemented in the 'ecospat' R package (Di Cola et al. 2017). We show all additional results from these robustness tests, including the above mentioned robust variable sets, in the supplementary material (Supplementary material Appendix 3). Because the alternative niche quantification approach did not reveal significant differences compared to our original hypervolume analyses, we here report the latter and refer the reader to the Supplementary material Appendix 3 for a detailed comparison of methods.

In addition to hypervolume construction, we used MaxEnt species distribution modeling (Elith et al. 2011, Renner and Warton 2013) as a predictive framework to infer niche breadth and geographic overlap of fungal and algal OTUs. MaxEnt is the most commonly used SDM algorithm that has been shown to perform well for datasets with few occurrence sample points (Elith et al. 2006, Phillips et al. 2006, Elith and Graham 2009, Allen and Lendemer 2016). All MaxEnt models were run for the basic set of 12 bioclim variables, the full set of 19 bioclim variables, and the set of seven bioclim variables that were the least correlated (see Supplementary material Appendix 2 for detailed results). To address issues of model complexity, overfitting, and evaluation, we first applied a jackknife data-partitioning approach to distribute occurrence and background localities (n = 5000) into training and testing bins for k – 1 crossvalidations of k occurrence localities (Shcheglovitova and Anderson 2013, Mateo et al. 2015). Different levels of model complexity were then explored across varying classes of response curves (L: linear, LQ: linear and quadratic, LQH: linear quadratic hinge, H: hinge, and LQHP: linear quadratic

hinge product) and regularization multipliers (ranging from 0.5–4), as implemented in the R packages 'dismo' and 'ENMeval' (Muscarella et al. 2014, Hijmans et al. 2015). From a total of 48 different parameter sets, we chose the best model complexity based on AICc values and the AUC criterion (Phillips et al. 2006, Warren and Seifert 2011). In addition to visualizing the predicted spatial distribution of OTUs, we used MaxEnt model outcomes to infer potential interaction hotspots, defined as geographic areas where the encounter probability of particular symbiont partners (i.e. their combined occurrence probabilities) is predicted to be high. Moreover, we calculated pairwise overlap scores for all mycobionts and photobionts in total niche space, based on Schoener's D (ranging from 0: no overlap, to 1: complete overlap; Schoener 1968). For both sets of analyses (hypervolumes and SDMs) we omitted OTUs with too few sampling locations (n < 5), or combined their distributions (see Results). All analyses were carried out in R 3.3.2 (R Core Development Team).

Data deposition

Results

Genetic structure and OTU delimitation

Most of the genetic variance among *Trebouxia* photobionts was detected within mycobionts (93.61%), whereas only 6.39% variation was explained between mycobionts (AMOVA), indicating that only a small fraction of the total variance among photobionts is structured by mycobiont partners. The spatial structure of ITS variation in photobionts across our sampling area, as described by the first MEMGENE axis (explaining 72% of the genetic variation) reveals the greatest differentiation between haplotypes occurring in central Europe and haplotypes from the Mediterranean regions, the British Isles, and south-eastern Europe (Fig. 1B). Comparing the amount of spatial genetic pattern explained by the full analysis ($R^2 = 16.31$) with recently published simulation results further indicates that more of the genetic structure in our data is explicable by spatial structure than might be expected under a pure isolation-by-distance (IBD) scenario where R^2 values typically fall below 0.10 (Galpern et al. 2014). For fungal haplotypes, spatial structuring of *MCM7* variation was non-significant (i.e. no significant MEMGENE axes found) and a low R^2 value of 0.06 did not exclude the IBD null model (distribution plot based on non-significant MEMGENE axis 1 is shown in Supplementary material Appendix 1 Fig. S1).

The two approaches to delineate clusters of genetic variance in mycobionts and photobionts yielded very similar results. For *Trebouxia* photobionts, the 42 ITS

haplotypes were grouped into seven distinct clusters based on hierarchical clustering of pairwise genetic distances. Using the alternative ABGD method (Puillandre et al. 2012), we recovered six OTUs (hereafter OTU$_{alga}$, based on JC69 distance model with prior maximal distance, p = 0.0046), one of which merged two of the aforesaid clusters (Supplementary material Appendix 1 Fig. S2A, Supplementary material Table S1). For the *L. pustulata* mycobiont, hierarchical clustering of 11 haplotypes yielded nine clusters, of which two were merged by the ABGD method into a total of seven OTUs (hereafter OTU$_{fungus}$, based on JC69 distance model with prior maximal distance, p = 0.0028; Supplementary material Appendix 1 Fig. S2B). Haplotype networks for photobionts and mycobionts respectively are shown in Supplementary material Appendix 1 Fig. S3. Furthermore, comparing the *Trebouxia* haplotypes from our study to the 69 ITS OTUs underlying the recently proposed classification system for *Trebouxia* photobionts (Leavitt et al. 2015) revealed that all of our haplotypes fall into the 'S' clade (*simplex/letharii/jamesii* group; Supplementary material Appendix 1 Fig. S2A). For downstream ecological analyses, we omitted algal and fungal OTUs with too few sampling locations (n < 5), leading to the exclusion of three mycobionts (OTU$_{fungus}$ 5–7), and one photobiont (OTU$_{alga}$ 6) for niche construction and SDM analyses (Supplementary material Table S1). In order to complete results for the omitted mycobionts, we also combined the distribution data of OTU$_{fungus}$ 5–7 and examined their merged niche dimensions.

Climatic niche construction and SDM

We constructed 2-dimensional (BioClim PC1–PC2; explaining 90% variation) hypervolumes for each OTU (i.e. the target OTU) versus all of the remaining OTUs combined. Inspection of overlaps between these two projections in PCA space allows the following interpretation regarding environmental preferences of target OTUs: in photobionts, we found the environmental preferences of OTU$_{alga}$ 1 to span most of the total *Trebouxia* niche space (here defined as the *Trebouxia* niche space in association with *L. pustulata* in our study), extending into all main climatic dimensions of the depicted PCA space (Fig. 2A). Two other OTU$_{alga}$, 2 and 3, showed restricted niche dimensions, and neither of them covered a unique area of the total *Trebouxia* niche. Interestingly, the two remaining OTU$_{alga}$ showed non-overlapping dimensions compared to the remaining overall niche projection (OTU$_{alga}$ 1–3), both at opposite ends of niche space: OTU$_{alga}$ 4 spreading uniquely into colder and wetter regions, and OTU$_{alga}$ 5 spreading uniquely into warmer and potentially drier regions (Fig. 2A). Applying the same logic to projections of OTU$_{fungus}$ niches revealed a different picture for the environmental preferences among the mycobionts. Here, OTU$_{fungus}$ 1 broadly covered the full *L. pustulata* niche space depicted in our study, including several unique portions (Fig. 2B). In contrast, the remaining four OTU$_{fungus}$ (2–4, and 5–7 merged) indeed showed differences in their niche dimensions, but none comprised unique (i.e. non-overlapping) portions

of the full niche projection, except a small fraction for OTU$_{fungus}$ 2 (Fig. 2B).

A similar picture emerged from MaxEnt SDM predictions. After evaluation of the best parameter sets for each OTU (Supplementary material Table S3), MaxEnt was run for OTUs (alga and fungus) with > 15 sampling locations. From this, we highlight SDM results for three OTU$_{alga}$ (1, 4, and 5) that already showed distinguished patterns of habitat suitability in hypervolume projections. In particular, the geographic SDM predictions for habitat suitability in OTU$_{alga}$ 1 confirmed its relatively generalistic climatic preferences (in association with *L. pustulata*), with the highest suitability values for central European regions, northern Spain, and northern Turkey (Fig. 3, upper panel). In contrast, OTU$_{alga}$ 4 had the highest suitability scores in arctic-alpine regions, such as the Alps, the Pyrenees, the Cantabrian mountain ridge, Scotland, and Norway. OTU$_{alga}$ 5, the putatively more warm-tolerant photobiont, was predicted to occur with the highest probability in the Mediterranean region (southern Spain, southern Italy, Corsica, Sardinia, and the Aegean Sea), as well as the Canary Islands (Fig. 3, upper panel). To further explore how these niche preferences in photobionts might translate into geographic hotspots of symbiotic interactions, we overlaid the SDM predictions for each of the three OTU$_{alga}$ (1, 4, and 5) with the overall SDM prediction for the mycobionts (combining predictions for all OTU$_{fungus}$). Using multiplication as the connecting operation between SDM prediction layers of symbiont partners then yielded a map of potential interaction hotspots where it is most likely that the (generalist) mycobiont overlaps with particular photobionts (depicted as encounter probability in Fig. 3, lower panel). In accordance with hypervolume projections and SDM model predictions, the OTU$_{fungus}$–OTU$_{alga}$–overlap quantification depicts interaction hotspots for OTU$_{alga}$ 1 (generalist) to be broadly distributed, hotspots for OTU$_{alga}$ 4 (cold preferring) located in colder regions and higher elevations, and hotspots for OTU$_{alga}$ 5 (warm preferring) in warmer Mediterranean regions and the Canary Islands (Fig. 3, lower panel). A complete overview of separate MaxEnt model projections for all OTUs with sufficient data is given in Supplementary material Appendix 1 Fig. S4, while Fig. S5 gives pairwise niche overlap scores between all OTU$_{alga}$ and OTU$_{fungus}$ based on Schoener's D metric.

Discussion

Theory predicts that mutualists may augment the environmental tolerance of host species and increase the potential for a host to expand its ecological niche and geographic range (Moran 2007, Poisot et al. 2011, Friesen and Jones 2012, Hussa and Goodrich-Blair 2013). Empirical examples come from fungal or bacterial symbionts that catalyse niche expansion in plants and invertebrates (Joy 2013, Afkhami et al. 2014, Chong and Moran 2016, Maher et al. 2017), or from photosynthetic algal symbionts that govern distinct environmental zonation in corals and sea anemones (Bates 2000,
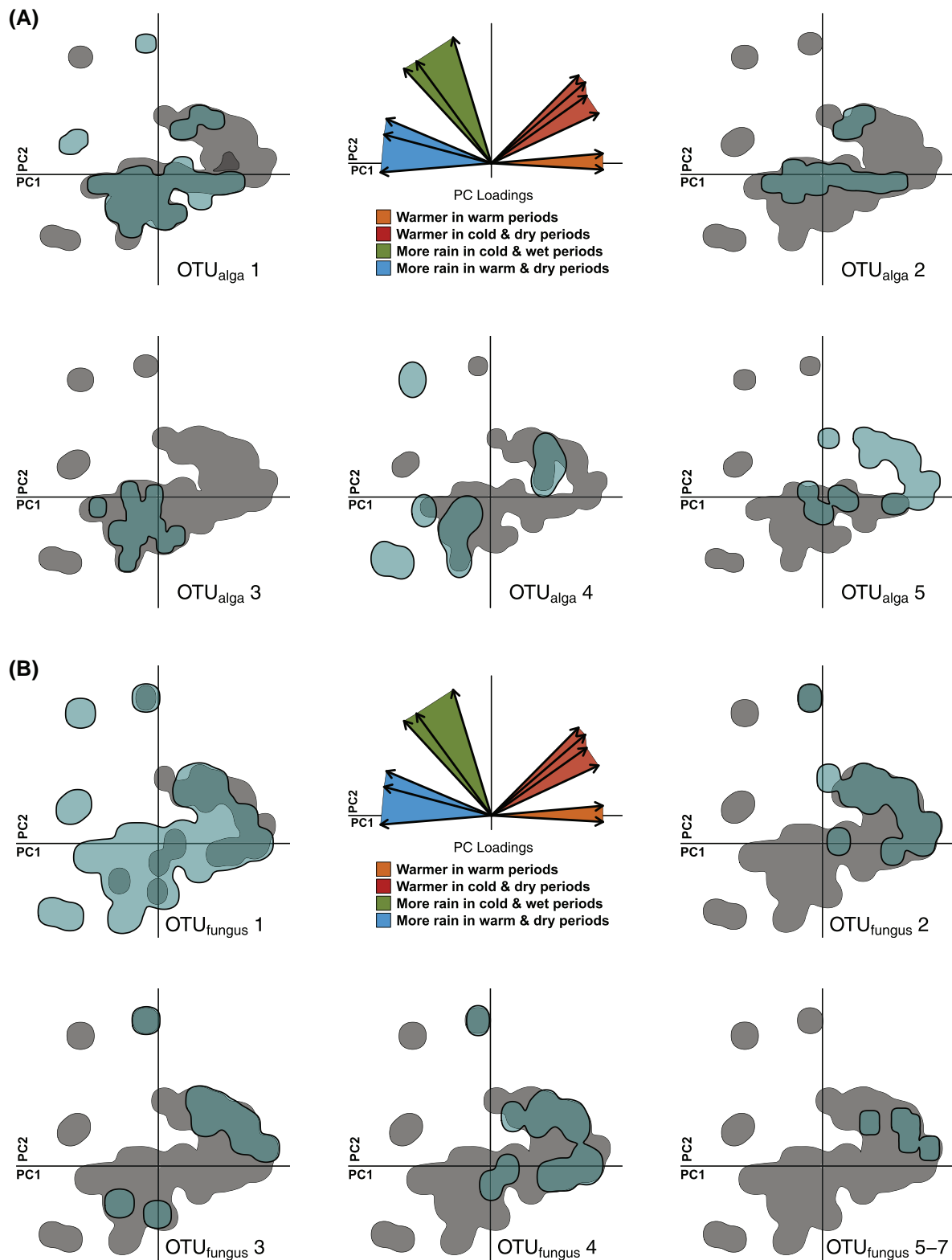
Figure 2. Niche hypervolumes for (A) *Trebouxia* photobionts and (B) *L. pustulata* mycobionts based on environmental PC1–PC2 axes (explaining 94% of variation; PC loadings are depicted in mid-upper panel together with their general interpretations; Supplementary material Table S2). Each of the five projections in (A) and (B) shows the niche hypervolume of a particular $OTU_{alga\ (A)/fungus\ (B)}$ (in cyan) superimposed on the complete niche hypervolume of all remaining $OTU_{alga/fungus}$ (in grey). Non-overlapping portions of cyan and grey projections indicate unique contributions of a particular OTU to the overall fungal or algal niche space.
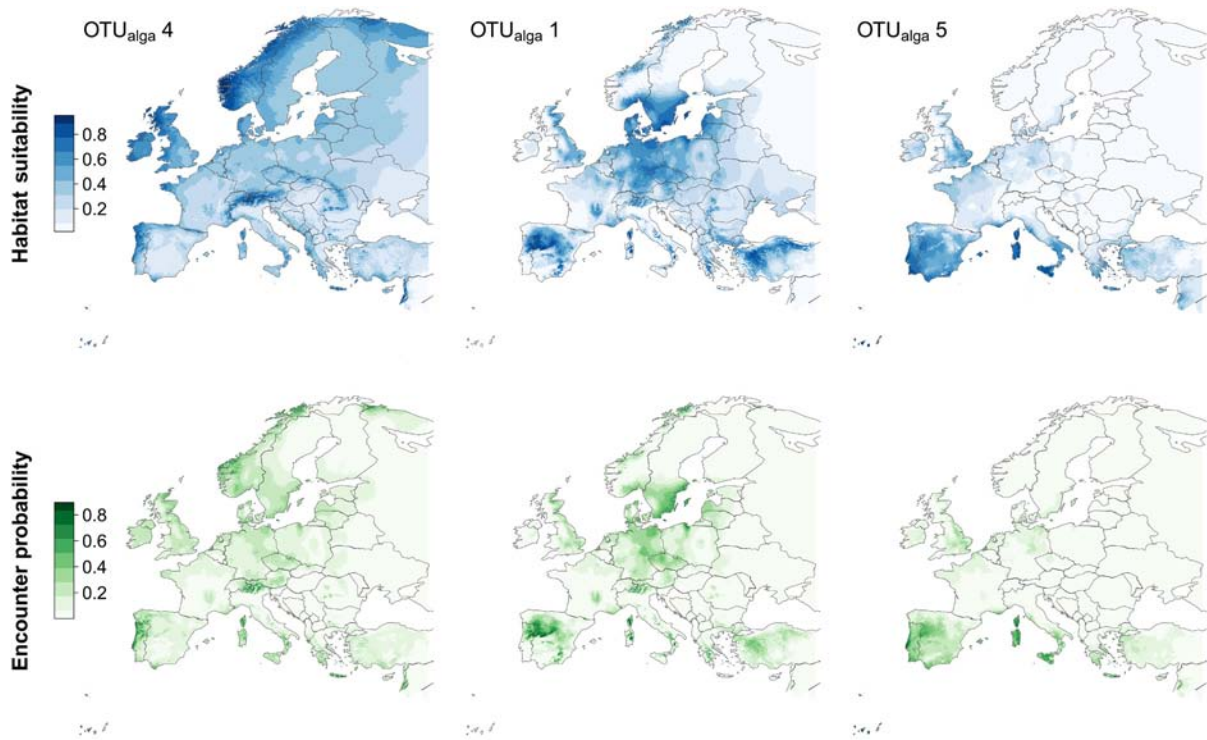
Figure 3. Upper panel: habitat suitability predictions from MaxEnt species distribution models for three prominent algal OTUs (generalistic ecotype OTU_{alga} 1, arctic-alpine ecotype OTU_{alga} 4, and Mediterranean ecotype OTU_{alga} 5). Lower panel: encounter probability of the above ecotypes with the fungal mycobiont (all OTU_{fungus}) throughout the distributional range of *L. pustulata*. Probability scores were calculated as the product of model-based habitat suitabilities for the respective photobionts (OTU_{alga} 1, 4, and 5) and the mycobiont (combining all OTU_{fungus}). Separate model predictions for all symbiont partners are depicted in Supplementary material Appendix 1 Fig. S4.

Iglesias-Prieto et al. 2004, Mieog et al. 2009, Bongaerts et al. 2015). Similar patterns are also observed in lichen symbioses where a particular mycobiont can associate with genetically differentiated photobionts across a broad eco-geographic range (Opanowicz and Grube 2004, Yahr et al. 2006, Muggia et al. 2010, Fernández-Mendoza et al. 2011, Werth and Sork 2014). Yet, to what extent ecological differentiation (e.g. climatic tolerance) among distinct mutualists alters the overall niche breadth of a symbiosis, is less well understood. To investigate this question, we quantified individual niche contributions of genetically differentiated photobionts and mycobionts in the lichen *L. pustulata* across its core range. The particular distribution pattern we found resembles a climatically structured interaction mosaic between symbionts, and highlights the association with different photobionts as an adaptive strategy in this lichen.

Genetic variance and spatial structure

All 42 *Trebouxia* algae haplotypes we found for our broad-scale European dataset (Fig. 1A) fall within the 'S' clade of the recently published *Trebouxia* phylogeny (Leavitt et al. 2015), where they mainly comprise two distinct clades together with the already existing stock of 'S'-clade photobionts. One of these clades includes OTU_{alga} 1, 3, and 6 – showing more generalistic environmental preferences; whereas the other

clade includes, along with OTU_{alga} 2, the two environmentally specialized OTU_{alga} 4, and 5 (Supplementary material Appendix 1 Fig. S2A). A closer look at the spatial distribution of ITS variance among photobionts reveals a central cluster, surrounded by a differentiated peripheral cluster (Fig. 1B). Regression modeling that involved spatially explicit predictors to explain genetic distances among photobiont haplotypes, further indicated that the basic negative relationship between distance and gene flow (isolation-by-distance, IBD) might not be sufficient to explain the genetic structure in our data. We thus interpret the pattern of spatial differentiation to be not only governed by IBD dynamics, but also by adaptive dynamics of particular photobionts evolving distinct environmental preferences. As for the mycobiont, we did not discover significant spatial structure in *MCM7* variation compared to ITS variation in photobionts (Supplementary material Appendix 1 Fig. S1). The analyses of spatial genetic variation among haplotypes of these markers therefore suggests environmental structuring in photobionts, but not in mycobionts; a pattern that was then further corroborated through niche modeling of algal and fungal OTUs.

Among the five photobiont OTUs that were further scrutinized for their environmental preferences (in association with *L. pustulata*), we found one generalist (OTU_{alga} 1) with a broad climatic niche, and two putative specialists (OTU_{alga} 4 and 5) with unique preferences at opposite ends of the

1387

climatic niche space governing our sampling area (Fig. 2A). Notably, although our delineation approach is based on only a single genetic marker, the barcode gap detection approach (ABGD, Puillandre et al. 2012) we applied to define OTUs has recently been tested extensively for *Trebouxia* algal ITS sequences where it reliably depicted OTU boundaries (Leavitt et al. 2015). Accordingly, we consider the photobiont OTUs recovered from our data as evolutionary independent, non-recombining units for which the described pattern of non-overlapping niches (in OTU_{alga} 4 and 5) suggests distinct climatic preferences in response to environmental selection (Graham et al. 2004, Kozak et al. 2008). However, for an in-depth examination of adaptive divergence among *Trebouxia* photobionts – which was not the focus of our study – the description of genetic variance has to include genome-wide patterns that surmount the scope of a single (or a few) barcode markers.

In comparison to the niche spaces we found for the photobionts of *L. pustulata*, the mycobionts showed a different pattern, involving a broadly distributed generalistic type (OTU_{fungus} 1) that occurred throughout the sampling area, together with a few genetically differentiated sub-types that did, however, not show unique climatic preferences in their spatial distributions (Fig. 2B). Interestingly, the selective regimes potentially associated with the genetic variation among photobionts lie on opposite ends of the full climatic spectrum of *L. pustulata* (Fig. 2A). Hence, variation in environmental preferences among algal OTUs significantly broadens the overall niche space of *L. pustulata* towards colder and wetter climates (OTU_{alga} 4 associating with OTU_{fungus} 1), as well as towards warmer and drier climates (OTU_{alga} 5 associating with OTU_{fungus} 1–4). Taken together, the analyses of spatial genetic variance and niche hypervolumes in *L. pustulata* lichens thus support the hypothesis of photobiont switches as an adaptive strategy for a (generalist) mycobiont to broaden its distributional range (Piercey-Normore and DePriest 2001, Werth and Sork 2008, 2010, Fernández-Mendoza et al. 2011, O'Brien et al. 2013).

Distribution modeling and interaction hotspots

Given that photobiont switches occur throughout the distributional range of *L. pustulata*, such that the generalist mycobiont will associate with locally frequent photobionts, the question then arises as to where these switches are most likely to take place. Based on species distribution models (SDM), we approached this question by translating environmental preferences of symbiont partners into their respective geographic distributions. With regard to algal switches and niche expansion, we focused on interactions between the generalist mycobiont and the three photobiont OTUs that showed either generalistic (OTU_{alga} 1), cold-tolerant (OTU_{alga} 4), or warm-tolerant (OTU_{alga} 5) distributions in their association with *L. pustulata*. In accordance with niche hypervolume analyses, SDMs predicted OTU_{alga} 1 to span most of central Europe, whereas habitat suitability for OTU_{alga} 4

peaked in arctic-alpine regions, and OTU_{alga} 5 appeared to be restricted to the Mediterranean (Fig. 3; Supplementary material Appendix 1 Fig. S4A). Moreover, as would be expected, SDMs for the mycobionts predicted a broad central European distribution with no particular specialization for OTU_{fungus} 1, and a clustered distribution in the Mediterranean region for OTU_{fungus} 2–4 (Supplementary material Appendix 1 Fig. S4B). We also point out that the suggested pattern of photobiont switches from the generalistic OTU_{alga} 1 to the warm preferring OTU_{alga} 5 in our broad-scale analyses has recently been detected along a local-scale altitudinal gradient in the Mediterranean (Dal Grande et al. 2017a; see Supplementary material Appendix 2 for congruency between OTU delimitations).

Interestingly, the overall distribution of suitable habitat for *Trebouxia* photobionts was predicted to be significantly larger than the overall distribution of *L. pustulata* mycobionts (Supplementary material Appendix 1 Fig. S4C). Here, it is important to note that the data only include *Trebouxia* strains that were found to be associated with *L. pustulata*, whereas other lichen-forming fungi occurring in the same range were not examined. Hence, given the low specificity of *Trebouxia* algae towards their fungal partners (Friedl and Büdel 1996, Piercey-Normore and DePriest 2001, Peksa and Škaloud 2011), we can currently not resolve whether the differentiated model distributions (and niches) of algal OTUs correspond to locally adapted strains, or whether their distributions are in fact broader considering additional fungal partners. In order to fully understand local adaptation in strains of lichen-associated algae, the spatial extent and dispersal capacities of the entire lichen community harboring those strains has to be taken into account.

Notwithstanding, the modeled distributions of algal OTUs from our data do strengthen the assumption that the range of *L. pustulata* lichens is probably not restricted, but broadened, by environmental preferences of *Trebouxia* algae. In particular, range expansions via photobiont switches will be most effective either towards colder and wetter climates, such as in arctic-alpine regions (switching to OTU_{alga} 4), or towards warmer and drier climates, such as in the Mediterranean (switching to OTU_{alga} 5, see also Dal Grande et al. 2017a). Accordingly, regarding the interaction hotspots of symbiont partners (depicted as the product of their respective occurrence probabilities), the generalist mycobiont (OTU_{fungus} 1) will also likely encounter these *Trebouxia* strains at the outer margins of its distribution (Fig. 3, lower panel). Notably, the remaining genetically differentiated mycobionts (OTU_{fungus} 2–4) primarily clustered in the Mediterranean (Supplementary material Appendix 1 Fig. S4B), suggesting diversification of mycobionts to be more likely in that region. However, to further explore the adaptive significance of this pattern, particularly in regard to photobiont switching and niche overlap (Supplementary material Appendix 1 Fig. S5), additional genome-wide analyses – as opposed to our rather conservative set of genetic markers (ITS rDNA for algae and *MCM7* for fungi) – would be valuable. For instance,

a recent study found genome-wide differentiation among *L. pustulata* mycobionts from the Mediterranean (Sardinia, Italy) that is likely driven by adaptive divergence along an elevational cline (Dal Grande et al. 2017b). Taken together, our results provide evidence for mutualist-mediated niche (and range) expansion in lichens – a strategy also observed in other mutualisms (Afkhami et al. 2014, Bongaerts et al. 2015, Maher et al. 2017) – thereby corroborating theoretical predictions for symbiosis as an adaptive process (Moran 2007, Poisot et al. 2011, Friesen and Jones 2012). We also highlight the importance of niche and distribution models to quantify or locate unique ranges and overlaps of distinct partners involved in a symbiosis (see also Peksa and Ŝkaloud 2011, Afkhami et al. 2014, Allen and Lendemer 2016).

Coevolution and ecological fitting

Regarding the underlying mechanisms structuring *L. pustulata* lichen symbioses across ecological gradients, the spatial genetic pattern of symbiont partners together with their model-based niche predictions can also help to distinguish between two fundamental mechanistic concepts of species associations: coevolution and ecological fitting. Coevolution requires reciprocal selection pressures between interacting species, such that the fitnesses of particular genotypes in one species depend on the distribution of genotypes in the other species (Ehrlich and Raven 1964, Thompson 1999, 2005). Moreover, this reciprocity in fitness functions will often be geographically structured based on local genotype-by-genotype-by-environment interactions, thereby creating a geographic mosaic of strong and weak (or absent) coevolution (Thompson 1999, 2005). On the one hand, strong interdependence of genotype distributions will lead to codiversification and phylogenetic conservatism among interacting partners. On the other hand, weak genetic interdependence can lead to breaks in codiversification, specifically if one genotype obtains realized fitness after colonizing a new habitat where fitnesses are not strongly dependent on the distribution of genotypes in the other species (Thompson 1999, Gomulkiewisz et al. 2000, Nuismer et al. 2000, 2003). The latter scenario is often related to the concept of ecological fitting which is based on the evolutionary history of interacting species being co-opted in a new selective environment with little to no adaptive divergence to the current partner (Janzen 1985, Agosta and Klemens 2008, Agosta et al. 2010).

The spatial genetic pattern we observed in *L. pustulata* lichens – i.e. a generalistic mycobiont switches between genetically differentiated photobionts with divergent ecological amplitudes – appears to be in agreement with the concept of ecological fitting, rather than with strong coevolution between specific genotypes. Indeed, our study thereby confirms a commonly observed pattern found in other lichen symbioses at the level of sub-species or populations (Piercey-Normore 2006, Yahr et al. 2006, Werth and Sork 2008, 2010, Muggia et al. 2014). On a larger phylogenetic scale, however, lichen symbioses are certainly structured by coevolution, as is evident from strong phylogenetic constraint in partner compatibility (DePriest 2004, Yahr et al. 2004, Miadlikowska et al. 2006, Leavitt et al. 2015, Singh et al. 2017). Interestingly, despite only weak codiversification among partners on the sub-species level, their spatial interaction pattern – especially in regard to niche expansion – will often still resemble a mosaic of interaction hotspots (where putatively specialized partners are more frequently available) and coldspots (where there are mainly generalist partners). Hence, it is important for our understanding of lichen symbioses to identify such hotspots where photobiont switches will most likely occur with adaptive benefits.

Conclusions

This study highlights the importance of spatial genetic approaches in order to determine the ecological drivers that structure mutualisms (Yahr et al. 2006, Werth and Sork 2008, 2010, Muggia et al. 2014). Our results confirm a commonly observed pattern in lichen symbioses, where a generalist mycobiont associates with genetically differentiated and ecologically divergent photobionts, thereby potentially expanding its distributional range. Particularly with regard to ongoing climate change, the identification of interaction hotspots among symbiont partners will not only help to understand how lichens can cope with shifting climatic selection regimes, but also to inform conservation strategies on potentially vulnerable populations (Klanderud and Totland 2005, Ellis 2012, Allen and Lendemer 2016). Importantly, given that our assessment of genetic differentiation is currently based on a rather conservative set of genetic markers (ITS rDNA for algae and *MCM7* for fungi), additional analyses with broad-scale genomic tools are needed. To conclude, quantifying the ecological contribution of different genotypes to the overall (climatic) niche of a symbiosis will help to inform future molecular and genomic approaches aiming to understand eco-evolutionary dynamics in mutualisms.

References

Afkhami, M. E. et al. 2014. Mutualist-mediated effects on species' range limits across large geographic scales. – Ecol. Lett. 17: 1265–1273.

Agosta, S. J. and Klemens, J. A. 2008. Ecological fitting by phenotypically flexible genotypes: implications for species associations, community assembly and evolution. – Ecol. Lett. 11: 1123–1134.

Agosta, S. J. et al. 2010. How specialists can be generalists: resolving the "parasite paradox" and implications for emerging infectious disease. – Zoologia 27: 151–162.

Allen, J. L. and Lendemer, J. C. 2016. Climate change impacts on endemic, high-elevation lichens in a biodiversity hotspot. – Biodivers. Conserv. 25: 555–568.

Bates, A. 2000. The intertidal distribution of two algal symbionts hosted by *Anthopleura xanthogrammica* (Brandt 1835). – J. Exp. Mar. Biol. Ecol. 249: 249–262.

Beck, A. et al. 1998. Selectivity of photobiont choice in a defined lichen community: inferences from cultural and molecular studies. – New Phytol. 139: 709–720.

Bjerke, J. W. 2011. Winter climate change: ice encapsulation at mild subfreezing temperatures kills freeze-tolerant lichens. – Environ. Exp. Bot. 72: 404–408.

Blaha, J. et al. 2006. High photobiont diversity associated with the euryoecious lichen-forming ascomycete *Lecanora rupicola* (Lecanoraceae, Ascomycota). – Biol. J. Linn. Soc. 88: 283–293.

Blonder, B. et al. 2014. The n-dimensional hypervolume. – Global Ecol. Biogeogr. 23: 595–609.

Bongaerts, P. et al. 2015. Prevalent endosymbiont zonation shapes the depth distributions of scleractinian coral species. – R. Soc. Open Sci. 2: 140297.

Borcard, D. and Legendre, P. 2002. All-scale spatial analysis of ecological data by means of principal coordinates of neighbour matrices. – Ecol. Model. 153: 51–68.

Brodie, E. D. et al. 2002. The evolutionary response of predators to dangerous prey: hotspots and coldspots in the geographic mosaic of coevolution between garter snakes and newts. – Evolution 56: 2067–2082.

Broennimann, O. et al. 2012. Measuring ecological niche overlap from occurrence and spatial environmental data. – Global Ecol. Biogeogr. 21: 481–497.

Chase, J. M. and Leibold, M. A. 2003. Ecological niches – linking classical and contemporary approaches. – Univ. of Chicago Press.

Chong, R. A. and Moran, N. A. 2016. Intraspecific genetic variation in hosts affects regulation of obligate heritable symbionts. – Proc. Natl Acad. Sci. USA 113: 13114–13119.

Crabtree, D. and Ellis, C. J. 2010. Species interaction and response to wind speed alter the impact of projected temperature change in a montane ecosystem. – J. Veg. Sci. 21: 744–760.

Cubero, O. F. and Crespo, A. 2002. Isolation of nucleic acids from lichens. – In: Kranner, I. C. et al. (eds), Protocols in lichenology. Springer, pp. 381–391.

Dal Grande, F. et al. 2012. Vertical and horizontal photobiont transmission within populations of a lichen symbiosis. – Mol. Ecol. 21: 3159–3172.

Dal Grande, F. et al. 2014. Molecular phylogeny and symbiotic selectivity of the green algal genus *Dictyochloropsis* s.l. (Trebouxiophyceae): a polyphyletic and widespread group forming photobiont-mediated guilds in the lichen family Lobariaceae. – New Phytol. 202: 455–470.

Dal Grande, F. et al. 2017a. Environment and host identity structure communities of green algal symbionts in lichens. – New Phytol. doi:10.1111/nph.14770

Dal Grande, F. et al. 2017b. Adaptive differentiation coincides with local bioclimatic conditions along an elevational cline in populations of a lichen-forming fungus. – BMC Evol. Biol. 17: 93.

DePriest, P. T. 2004. Early molecular investigations of lichen-forming symbionts: 1986–2001. – Annu. Rev. Microbiol. 58: 273–301.

Di Cola, V. et al. 2017. Ecospat: an R package to support spatial analyses and modeling of species niches and distributions. – Ecography 40: 774–787.

Doering, M. and Piercey-Normore, M. D. 2009. Genetically divergent algae shape an epiphytic lichen community on Jack Pine in Manitoba. – Lichenology 41: 69–80.

Dormann, C. F. et al. 2013. Collinearity: a review of methods to deal with it and a simulation study evaluating their performance. – Ecography 36: 27–46.

Dray, S. et al. 2012. Community ecology in the age of multivariate multiscale spatial analysis. – Ecol. Monogr. 82: 257–275.

Ehrlich, P. R. and Raven, P. H. 1964. Butterflies and plants: a study in coevolution. – Evolution 18: 586–608.

Elith, J. and Graham, C. H. 2009. Do they? How do they? WHY do they differ? On finding reasons for differing performances of species distribution models. – Ecography 32: 66–77.

Elith, J. et al. 2006. Novel methods improve prediction of species' distributions from occurrence data. – Ecography 29: 129–151.

Elith, J. et al. 2011. A statistical explanation of MaxEnt for ecologists. – Divers. Distrib. 17: 43–57.

Ellis, C. J. 2012. Lichen epiphyte diversity: a species, community and trait-based review. – Perspect. Plant Ecol. Evol. Syst. 14: 131–152.

Ellis, C. J. et al. 2014. Response of epiphytic lichens to 21st century climate change and tree disease scenarios. – Biol. Conserv. 180: 153–164.

Excoffier, L. et al. 1992. Analysis of molecular variance inferred from metric distances among DNA haplotypes: application to human mitochondrial DNA restriction data. – Genetics 131: 479–491.

Fernández-Mendoza, F. et al. 2011. Population structure of mycobionts and photobionts of the widespread lichen *Cetraria aculeata*. – Mol. Ecol. 20: 1208–1232.

Friedl, T. 1987. Thallus development and phycobionts of the parasitic lichen *Diploschistes muscorum*. – Lichenology 19: 183–191.

Friedl, T. and Büdel, B. 1996. Photobionts. – In: Nash, T. H. (ed.), Lichen biology. Cambridge Univ. Press, pp. 8–23.

Friesen, M. L. and Jones, E. I. 2012. Modelling the evolution of mutualistic symbioses. – In: van Helden, J. et al. (eds), Bacterial molecular networks. Springer, pp. 481–499.

Galpern, P. et al. 2014. MEMGENE: Spatial pattern detection in genetic distance data. – Methods Ecol. Evol. 5: 1116–1120.

Gomulkiewicz, R. et al. 2000. Hot spots, cold spots, and the geographic mosaic theory of coevolution. – Am. Nat. 156: 156–174.

Gotelli, N. J. and Stanton-Geddes, J. 2015. Climate change, genetic markers and species distribution modelling. – J. Biogeogr. 42: 1577–1585.

Graham, C. H. et al. 2004. Integrating phylogenetics and environmental niche models to explore speciation mechanisms in dendrobatid frogs. – Evolution 58: 1781–1793.

Griffith, D. A. and Peres-Neto, P. R. 2006. Spatial modeling in ecology: the flexibility of eigenfunction spatial analyses. – Ecology 87: 2603–2613.

Guisan, A. and Zimmermann, N. E. 2000. Predictive habitat distribution models in ecology. – Ecol. Model. 135: 147–186.

Hebert, P. D. N. et al. 2003. Biological identifications through DNA barcodes. – Proc. R. Soc. B 270: 313–321.

Hijmans, R. J. et al. 2005. Very high resolution interpolated climate surfaces for global land areas. – Int. J. Climatol. 25: 1965–1978.

Hijmans, R. J. et al. 2015. dismo: species distribution modeling. – R package ver. 1.0-12. <http://cran.r-project.org>.

Hussa, E. A. and Goodrich-Blair, H. 2013. It takes a village: ecological and fitness impacts of multipartite mutualism. – Annu. Rev. Microbiol. 67: 161–178.

Hutchinson, G. 1957. Concluding remarks. – Cold Spring Harb. Symp. Quant. Biol. 22: 415–427.

Iglesias-Prieto, R. et al. 2004. Different algal symbionts explain the vertical distribution of dominant reef corals in the Eastern Pacific. – Proc. R. Soc. B 271: 1757–1763.

Janzen, D. H. 1985. On ecological fitting. – Oikos 45: 308–310.

Joy, J. B. 2013. Symbiosis catalyses niche expansion and diversification. – Proc. R. Soc. B 280: 20122820.

Keaney, M. 2006. Habitat, environment and niche: what are we modelling? – Oikos 115: 186–191.

Klanderud, K. and Totland, O. 2005. Simulated climate change altered dominance hierarchies and diversity of an alpine biodiversity hotspot. – Ecology 86: 2047–2054.

Kozak, K. H. et al. 2008. Integrating GIS-based environmental data into evolutionary biology. – Trends Ecol. Evol. 23: 141–148.

Kroken, S. and Taylor, J. W. 2000. Phylogenetic species, reproductive mode, and specificity of the green alga Trebouxia forming lichens with the fungal genus Letharia. – Bryologist 103: 645–660.

Leavitt, S. D. et al. 2015. Fungal specificity and selectivity for algae play a major role in determining lichen partnerships across diverse ecogeographic regions in the lichen-forming family Parmeliaceae (Ascomycota). – Mol. Ecol. 24: 3779–3797.

Lendemer, J. C. and Allen, J. L. 2014. Lichen biodiversity under threat from sea-level rise in the Atlantic Coastal Plain. – Bioscience 64: 923–931.

Maher, A. M. D. et al. 2017. An entomopathogenic nematode extends its niche by associating with different symbionts. – Microb. Ecol. 73: 211–223.

Manel, S. et al. 2012. Broad-scale adaptive genetic variation in alpine plants is driven by temperature and precipitation. – Mol. Ecol. 21: 3729–3738.

Marcer, A. et al. 2016. Geographical restructuring of Arabidopsis thaliana's genetic makeup in the Iberian Peninsula due to climate change based on genetic cluster membership. – BioRxiv <http://dx.doi.org/10.1101/091686>.

Mateo, R. G. et al. 2015. What is the potential of spread in invasive bryophytes? – Ecography 38: 480–487

Miadlikowska, J. et al. 2006. New insights into classification and evolution of the Lecanoromycetes (Pezizomycotina, Ascomycota) from phylogenetic analyses of three Ribosomal RNA- and two protein-coding genes. – Mycologia 98: 1088–1103.

Mieog, J. C. et al. 2009. The roles and interactions of symbiont, host and environment in defining coral fitness. – PLoS One 4: e6364.

Moran, N. A. 2007. Symbiosis as an adaptive process and source of phenotypic complexity. – Proc. Natl Acad. Sci. USA 104: 8627–8633.

Muggia, L. et al. 2010. Morphological and phylogenetic study of algal partners associated with the lichen-forming fungus Tephromela atra from the Mediterranean region. – Symbiosis 51: 149–160.

Muggia, L. et al. 2014. Photobiont selectivity leads to ecological tolerance and evolutionary divergence in a polymorphic complex of lichenized fungi. – Ann. Bot. 114: 463–475.

Mukhtar, A. et al. 1994. Does the lichen alga Trebouxia occur free-living in nature: further immunological evidence. – Symbiosis 17: 247–253.

Muscarella, R. et al. 2014. ENMeval: an R package for conducting spatially independent evaluations and estimating optimal model complexity for Maxent ecological niche models. – Methods Ecol. Evol. 5: 1198–1205.

Nuismer, S. L. et al. 2000. Coevolutionary clines across selection mosaics. – Evolution 54: 1102–1115.

Nuismer, S. L. et al. 2003. Coevolution in temporally variable environments. – Am. Nat. 162: 195–204.

O'Brien, H. E. et al. 2013. Assessing population structure and host specialization in lichenized cyanobacteria. – New Phytol. 198: 557–566.

Opanowicz, M. and Grube, M. 2004. Photobiont genetic variation in Flavocetraria nivalis from Poland (Parmeliaceae, lichenized Ascomycota). – Lichenology 36: 125–131.

Peksa, O. and Ŝkaloud, P. 2011. Do photobionts influence the ecology of lichens? A case study of environmental preferences in symbiotic green alga Asterochloris (Trebouxiophyceae). – Mol. Ecol. 20: 3936–3948.

Phillips, S. J. et al. 2006. Maximum entropy modeling of species geographic distributions. – Ecol. Model. 190: 231–259.

Piercey-Normore, M. D. 2006. The lichen-forming ascomycete Evernia mesomorpha associates with multiple genotypes of Trebouxia jamesii. – New Phytol. 169: 331–344.

Piercey-Normore, M. D. and DePriest, P. T. 2001. Algal switching among lichen symbioses. – Am. J. Bot. 88: 1490–1498.

Poisot, T. et al. 2011. A conceptual framework for the evolution of ecological specialisation. – Ecol. Lett. 14: 841–851.

Puillandre, N. et al. 2012. ABGD, automatic barcode gap discovery for primary species delimitation. – Mol. Ecol. 21: 1864–1877.

Qaio, H. et al. 2016. A cautionary note on the use of hypervolume kernel density estimators in ecological niche modelling. – Global Ecol. Biogeogr. 26: 1066–1070.

Rambold, G. et al. 1998. Photobionts in lichens: possible indicators of phylogenetic relationships – Bryologist 101: 392–397.

Renner, I. W. and Warton, D. I. 2013. Equivalence of MAXENT and Poisson point process models for species distribution modeling in ecology. – Biometrics 69: 274–281.

Rikkinen, J. et al. 2002. Lichen guilds share related cyanobacterial symbionts. – Science 297: 357.

Roffler, G. H. et al. 2016. Identification of landscape features influencing gene flow: how useful are habitat selection models? – Evol. Appl. 9: 805–817.

Rolshausen, G. et al. 2017. Data from: Quantifying the climatic niche of symbiont partners in a lichen symbiosis indicates mutualist-mediated niche expansions. – Dryad Digital Repository, <http://dx.doi.org/10.5061/dryad.64149>.

Sadowska-Deś, A. D. et al. 2013. Assessing intraspecific diversity in a lichen-forming fungus and its green algal symbiont: evaluation of eight molecular markers. – Fungal Ecol. 6: 141–151.

Sadowska-Deś, A. D. et al. 2014. Integrating coalescent and phylogenetic approaches to delimit species in the lichen photobiont *Trebouxia*. – Mol. Phylogenet. Evol. 76: 202–210.

Schmitt, I. et al. 2009. New primers for promising single-copy genes in fungal phylogenetics and systematics. – Persoonia 23: 35–40.

Schoener, T. W. 1968. The *Anolis* lizards of Bimini: resource partitioning in a complex fauna. – Ecology 49: 704–726.

Shcheglovitova, M. and Anderson, R. P. 2013. Estimating optimal complexity for ecological niche models: a jackknife approach for species with small sample sizes. – Ecol. Model. 269: 9–17.

Singh, G. et al. 2017. Fungal–algal association patterns in lichen symbiosis linked to macroclimate. – New Phytol. 214: 317–329.

Thompson, J. N. 1999. Specific hypotheses on the geographic mosaic of coevolution. – Am. Nat. 153: S1–S14.

Thompson, J. N. 2005. The geographic mosaic of coevolution. – Univ. of Chicago Press.

Wagner, H. H. and Fortin, M. J. 2013. A conceptual framework for the spatial analysis of landscape genetic data. – Conserv. Genet. 14: 253–261.

Warren, D. L. and Seifert, S. N. 2011. Ecological niche modeling in Maxent: the importance of model complexity and the performance of model selection criteria. – Ecol. Appl. 21: 335–342.

Werth, S. and Sork, V. L. 2008. Local genetic structure in a North American epiphytic lichen, *Ramalina menziesii* (Ramalinaceae). – Am. J. Bot. 95: 568–576.

Werth, S. and Sork, V. L. 2010. Identity and genetic structure of the photobiont of the epiphytic lichen *Ramalina menziesii* on three oak species in southern California. – Am. J. Bot. 97: 821–830.

Werth, S. and Sork, V. L. 2014. Ecological specialization in *Trebouxia* (Trebouxiophyceae) across six range-covering ecoregions of western North America. – Am. J. Bot. 101: 1127–1140.

Widmer, I. et al. 2012. European phylogeography of the epiphytic lichen fungus *Lobaria pulmonaria* and its green algal symbiont. – Mol. Ecol. 21: 5827–5844.

Wirtz, N. et al. 2003. Lichen fungi have low cyanobiont selectivity in maritime Antarctica. – New Phytol. 160: 177–183.

Yahr, R. et al. 2004. Strong fungal specificity and selectivity for algal symbionts in Florida scrub *Cladonia* lichens. – Mol. Ecol. 13: 3367–3378.

Yahr, R. et al. 2006. Geographic variation in algal partners of *Cladonia subtenuis* (Cladoniaceae) highlights the dynamic nature of a lichen symbiosis. – New Phytol. 171: 847–860.

Supplementary material and GenBank accession numbers (Appendix ECOG-03457 at < www.ecography.org/appendix/ecog-03457 >). Appendix 1–4.